Molecular Simulations of Halomethanes at the Air/Ice Interface

ARTICLE *in* THE JOURNAL OF PHYSICAL CHEMISTRY A · SEPTEMBER 2015

Impact Factor: 2.69 · DOI: 10.1021/acs.jpca.5b06071 · Source: PubMed

THE JOURNAL OF PHYSICAL CHEMISTRY A

Article

pubs.acs.org/JPCA

Molecular Simulations of Halomethanes at the Air/Ice Interface

A. Habartová,[†] L. Hormain,[‡] E. Pluhařová,[†,§] S. Briquez,[‡] M. Monnerville,[‡] C. Toubin,*[,‡] and M. Roeselová[†]

[†]Institute of Organic Chemistry and Biochemistry, Academy of Sciences of the Czech Republic, Flemingovo nám. 2, 16610 Prague 6, Czech Republic

[‡]PhLAM Laboratory, UMR CNRS 8523, Université de Lille, Cité Scientifique, 59655 Villeneuve d'Ascq, France

[§]Department of Chemistry, École Normale Supérieure, UMR ENS-CNRS-UPMC 8640, 24 rue Lhomond, 75005 Paris, France

ABSTRACT: Halogenated organics are emitted into the atmosphere from a variety of sources of both natural and anthropogenic origin. Their uptake at the surface of aerosols can affect their reactivity, for example, in processes that take part in ozone destruction due to production of reactive chlorine, bromine, and iodine radicals. Classical molecular dynamics (MD) simulations are carried out to investigate the interaction of small halomethane molecules of atmospheric relevance with a crystalline ice surface. The following halomethanes were studied: CH_3Cl, CH_2Cl_2, $CHCl_3$, CH_3Br, CH_2Br_2, and $CHBr_3$. MD simulations provide an invaluable insight into the adsorption behavior of halomethanes species. The adsorption energy is increasing as the number of halogen atoms is increasing. Moreover, brominated methanes exhibit a stronger interaction with the ice than their chlorinated analogs. Implications for the atmospheric chemistry are discussed.

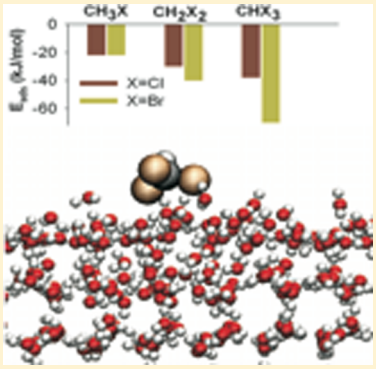

INTRODUCTION

There are still many open questions about the activation of halogens in the Polar Boundary Layer and its implication in the strastospheric ozone loss. The reviews by Saiz Lopez and Glasow[1] and Abbatt et al.[2] give a comprehensive account for the halogen activation in environmental ice and snow. Recent studies have shown that halocarbons are also important contributors to stratospheric bromine or chlorine loading, through their transport and photodegradation.[3,4] Volatile halogenated compounds were also measured in the water column, in the air and in sea ice brine across the Arctic Ocean.[5−7]

CH_3Cl is a naturally occurring, ozone-depleting trace gas and one of the most abundant chlorinated compounds in the atmosphere.[8] The relatively long tropospheric lifetime of CH_3Cl (>1 year) results in a significant amount of CH_3Cl being transported into the stratosphere, where it undergoes photolysis or reactions with OH radical to release ozone-destroying Cl atoms or convert to the temporary reservoirs of HCl, $ClONO_2$, and HOCl.[9]

By contrast, CHX_3 and CH_2X_2 (X = Cl or Br) have shorter lifetimes in the troposphere—with lifetimes <6 months—and are thus called very short lived species (VSLS). The most abundant chlorinated VSLS are CH_2Cl_2 and $CHCl_3$ for which anthropogenic activity accounts for 90% and 25%, respectively, of their tropospheric abundances. Indeed, there is an observed growth of tropospheric CH_2Cl_2 that could be due, in particular, to its use as a feedstock in the production of HFCs, the second generation of CFC replacement gases.[4]

The contribution of bromocarbons has also been increasingly recognized, especially given the enhanced ozone destruction potential of bromine in the lower stratosphere[3] which is 2 orders of magnitude higher than that of chlorine.

One pioneering experimental work[10] studied, by infrared spectroscopy (IR), the series of 23 halocarbon compounds interacting with water ice at 12 K. Perturbations to the water (D_2O) sites that are not saturated (dangling atoms) in the absence of guest molecules showed distinct trends (shifts of the dangling bond spectral position) depending on the type and extent of halogen substitution in the occluded molecules. IR spectroscopy was also used to investigate the ozonation of chlorinated methanes on polycrystalline ice over the temperature range 77−292 K.[11] Ozonation was observed at temperatures higher than 210 K under the conditions of the model experiments with an effective ozone destruction and formation of chlorine oxides.

The chemical sputtering technique has been used to investigate the diffusive mixing of chloromethanes in different molecular solids H_2O, D_2O, and CH_3OH, focusing on amorphous solid water.[12] It has been found that although the diffusion of CCl_4 in amorphous solid water (ASW) is hindered, other chloromethanes such as $CHCl_3$ and CH_2Cl_2 undergo diffusive mixing over the same temperature range.

By contrast, the adsorption of trichloromethane ($CHCl_3$) on ice layers has been studied extensively by various experimental techniques: temperature-programmed desorption (TPD), infrared reflection absorption spectroscopy (IRAS),[13] X-ray photoemission spectroscopy (XPS),[5] metastable impact electron

Received: June 24, 2015
Revised: August 26, 2015
Published: September 3, 2015

DOI: 10.1021/acs.jpca.5b06071
J. Phys. Chem. A 2015, 119, 10052−10059

spectroscopy.[14] It was found that the interaction of $CHCl_3$ with the ice is relatively weak and physisorptive, as expected from a hydrophobic nature of the molecule. The mobilities of tribromomethane ($CHBr_3$) and trichloromethane ($CHCl_3$) on amorphous solid water and crystalline ice surfaces have been compared using TPD spectroscopy and reflection absorption infrared spectroscopy.[15] The experiments concluded that $CHBr_3$ is more strongly bound than $CHCl_3$, as evidenced by its higher desorption temperature. Nevertheless, they also observed a lower barrier for surface diffusion of CH_3Br compared to that for $CHCl_3$. Computer calculations as those carried out in the present study will provide quantitative estimates of these interactions.

From a theoretical point of view, the halomethanes have received less attention than HCl and HBr, whose interaction with the ice surface has been extensively studied in the context of stratospheric ozone loss.[2] Theoretical studies were actually carried out on the CH_3X-H_2O dimer. One ab initio study characterized the geometry and binding energy of the $CH_xCl_{4-x}-H_2O$ dimer (x = 0, ..., 3).[16] The bromomethane–water 1:2 complexes have been also studied with the second-order Møller–Plesset theory (MP2) to reveal the role of hydrogen bond and halogen bond in the formation of different aggregates.[17] More recently, free energy profiles associated with the transfer of chlorinated and brominated halomethane molecules across the vapor–liquid water interface were calculated using classical molecular dynamics simulations.[18] To improve our understanding of the role of "hydration" for the removal of inorganic bromine or chlorine from the troposphere to the stratosphere, it is, therefore, crucial to further extend our knowledge about surface and uptake processes of haloalkanes at the ice surface. In this context, we have investigated by means of classical molecular dynamics simulation the interaction of the series of halomethanes ($CH_{4-n}X_n$, n = 1–3, X = Cl, Br) with a model crystalline ice surface. The MD simulation results provide molecular-level insight into the adsorption behavior and residence time of halomethane species contributing to a better understanding of some heterogeneous chemical processes in the atmosphere.

COMPUTATIONAL DETAILS

Molecular dynamics simulations of the halomethanes adsorption at T = 235 K were performed for a hexagonal (I_h) ice slab with the basal (0001) facet exposed to the vapor phase. For the halomethane molecules ($CH_{4-n}X_n$, n = 1–3, X = Cl, Br), the general Amber force field (GAFF) parameters set was employed. The atomic partial charges of the halomethane molecules along with the rest of the force field parameters are given in our previous work.[18] Water molecules were described using the TIP4P/2005 model.[19] The ice sample, consisting of 1344 water molecules, was constructed as an ideal ice crystal at 0 K using the algorithm of Buch et al.,[20] which yields a proton-disordered ice structure satisfying the Bernal–Fowler rules.[21] The dimensions of the initial ice sample were approximately 26.9 × 31.0 × 46.5 Å^3 in the x, y, and z directions, respectively. To equilibrate the ice to the target temperature, periodic boundary conditions were applied in all three dimensions, and a 200 ps isobaric–isothermal (NPT) simulation of bulk ice was performed. The ice sample was first annealed from 0 to 235 K over the course of 130 ps and then equilibrated at T = 235 K for an additional 70 ps. The Berendsen weak-coupling scheme[22] with time constants for heat bath coupling and pressure relaxation of 0.1 and 0.5 ps, respectively, was employed to control the temperature and pressure in the annealing and equilibration run. Once the ice–vacuum interface has been generated, the pressure of the barostat was set to zero to avoid the creation of a stress on the equilibrated structure.[23]

After equilibration of the ice bulk sample at the desired temperature, the z-dimension of the simulation cell was extended to 160 Å, resulting in an ice slab with two flat ice–vacuum interfaces located in the middle of the simulation cell, with a layer of vacuum on each side. The thickness of the ice slab was approximately 47 Å, corresponding to 14 ice crystal bilayers. The z axis is normal to the ice–vacuum interface. Two halocarbon molecules ($CH_{4-n}X_n$, n = 1–3, X = Cl, Br) were then added to the simulation cell, one to each of the two ice surfaces, at randomly selected x and y positions, and about 10 Å away from the ice surface along the z coordinate. The haloalkane molecules were assigned a small initial velocity (sampled randomly from the Maxwell–Boltzmann distribution corresponding to T = 10 K) pointing toward the respective ice surface. For each of the halomethanes species, the system was propagated for 50 ns in an isochoric–isothermal (NVT) ensemble at T = 235 K to sample structural and dynamical characteristics of the adsorbed halomethanes. The first 2 ns of each trajectory were excluded from analysis to allow the formation and equilibration of the disordered interfacial layer on the free basal planes of the ice slab. In the production run, the system's temperature was controlled by the Bussi–Donadio–Parrinello thermostat (velocity rescaling with a stochastic term)[24] with a coupling time of 0.5 ps. The melting point of the TIP4P/2005 model being $T_m \sim 250$ K,[23] the simulation at T = 235 K therefore corresponds to a 15 K undercooling with respect to the melting point of the model ice ($T = T_m - 15$ K).

All molecular dynamics calculations were performed using the GROMACS[25] (version 4.5.3) program package. The equations of motion were integrated by the leapfrog algorithm[26] with a 1 fs time step. The twin range cutoff scheme was employed, and both the Lennard-Jones and the short-range part of the Coulomb interactions were smoothly truncated to zero between 7 and 9 Å. The long-range part of the Coulomb interaction was evaluated using the smooth particle-mesh Ewald method[27,28] with a relative tolerance of 10^{-5}, fourth-order cubic interpolation and a Fourier spacing parameter of 0.12. Water molecules were treated as rigid bodies using SETTLE,[29] whereas no constraint was applied to the halomethane molecules. System configurations were saved at 1 ps intervals. Analysis of the trajectories was done using GROMACS tools, and the VMD program[30] was used for visualization.

RESULTS

All halomethane molecules ($CH_{4-n}X_n$, n = 1–3, X = Cl, Br) stick to the ice surface and remain adsorbed for the duration of the simulation. The adsorption properties are characterized in terms of configuration, orientation, bonding properties, and interaction energies.

1. Configuration of the Admolecule. Figure 1 shows some typical configurations obtained from the MD trajectory for each halomethane adsorbed at the gas/ice interfaces. From these snapshots, we can notice that in the simulated conditions (T = 235 K, T = T_m − 15 K) only the outermost interfacial layer of ice exhibits substantial disorder. All halomethane molecules are adsorbed on the top of the ice surface but with

DOI: 10.1021/acs.jpca.5b06071
J. Phys. Chem. A 2015, 119, 10052–10059

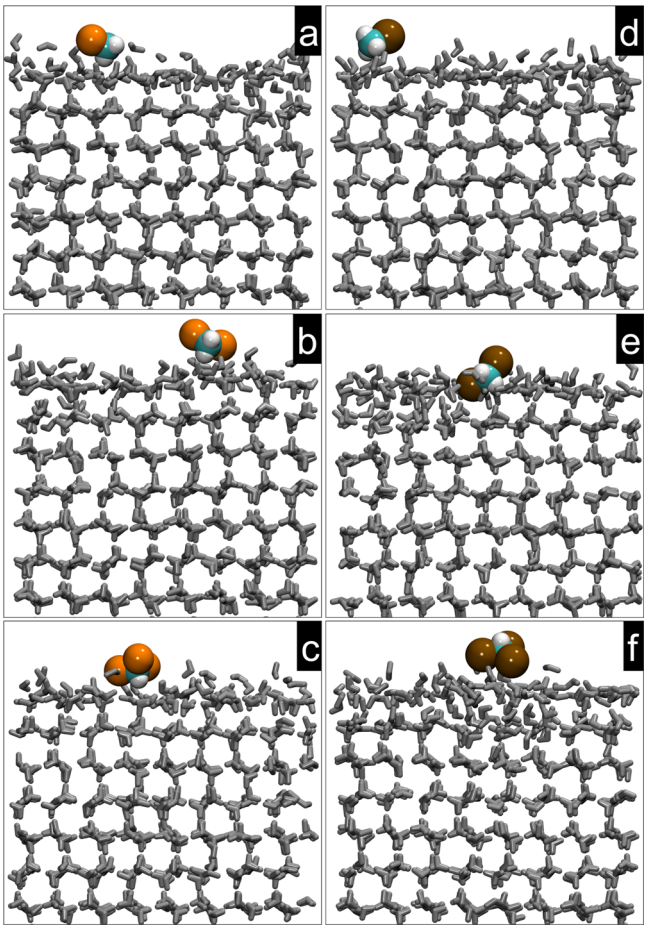

Figure 1. Side views of snapshots obtained from the MD simulation showing only the upper ice interface and the adsorbed halomethane with the corresponding legend: (a) CH_3Cl, (b) CH_2Cl_2, (c) $CHCl_3$, (d) CH_3Br, (e) CH_2Br_2, (f) $CHBr_3$. For clarity, the water molecules are represented by bonds. The halogen atoms, Cl and Br, are represented by orange and brown balls, respectively.

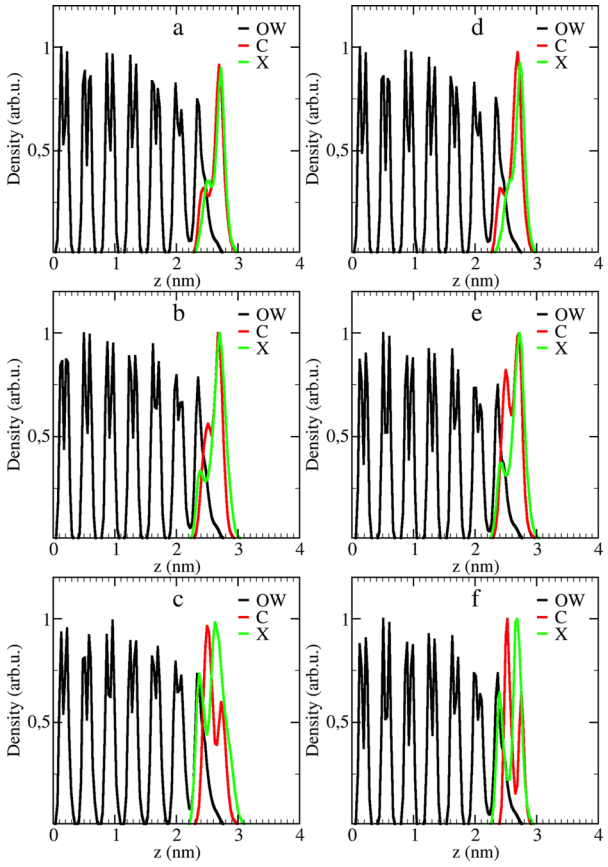

Figure 2. Density profiles along the z axis perpendicular to the interface for the oxygen atoms of water (black line), the carbon (red line) and halogen atoms (green line) of (a) CH_3Cl, (b) CH_2Cl_2, (c) $CHCl_3$, (d) CH_3Br, (e) CH_2Br_2, and (f) $CHBr_3$. For clarity, only the upper interface is shown. In each panel, the density curves have been normalized to their respective maximum peak for a better representation.

orientations and distances to the surface layer that differ from one to the other.

This qualitative view of the system can be rationalized by analyzing the density profiles of relevant atoms along the normal (z) to the ice surface. This is illustrated in Figure 2. The water oxygen density profiles are represented for simulations with all six halomethane admolecules, and they exhibit only minor differences. The inner layers of the ice slab are well ordered as evidenced by the double peaks corresponding to the water bilayers of the ice crystal lattice. The disappearance of the double peak for the outermost layer on both sides of the ice slab is a sign of a translational disorder of water molecules at the interface.

Considering the adsorption of the halomethane molecules, the methyl chloride and methyl bromide (Figures 2a,b) density profiles shapes are very similar to each other. The carbon density profiles exhibit a two-component signature: a sharp peak at about 2 Å from the surface water oxygen layer and a shoulder, less pronounced, corresponding to the admolecule incorporated deeper in the outermost ice layer. The chlorine density profile of CH_3Cl (Figure 2a) is almost completely superimposed onto the carbon one, indicating that methyl chloride is adsorbed nearly flat on the surface. The "outer" peak being more intense than the one relative to the "buried" site indicates that the more loosely physisorbed outer configuration is favored over the duration of the simulation. For CH_3Br (Figure 2d), the bromine density profile is also very close to the carbon one for the surface state. The fact that the bromine density is not so clearly superimposed to the carbon one, compared to the case for CH_3Cl, suggests a slightly more tilted orientation (with respect to the surface normal) for CH_3Br than for CH_3Cl.

For the dihalogenated methanes (Figure 2b,e), the carbon density profile resembles the ones of CH_3Cl or CH_3Br with the evidence of two types of adsorption sites. The halogen atoms are distributed on both sides of the carbon atoms, which can be interpreted in terms of two orientations: one with the C−Cl axis pointing toward the surface, and the other one nearly parallel to the surface (see next section). For CH_2Br_2, the carbon atom can occupy two positions at the ice surface with nearly the same probability, by contrast with CH_2Cl_2, CH_3Cl, and CH_3Br, where the carbon tends to be adsorbed predominantly in the site located at a larger distance from the surface layer.

The trihalogenated compounds (Figure 2c,f) have similar behaviors with two preferential positions of the carbon at the interface. However, the carbon and halogen density profiles indicate some differences between the trichloro- and tribromomethane. For $CHCl_3$, the carbon is essentially pointing toward

DOI: 10.1021/acs.jpca.5b06071
J. Phys. Chem. A 2015, 119, 10052−10059

the film and the chlorine atoms directed toward the vapor phase. By contrast, $CHBr_3$'s atomic distributions exhibit narrower peaks especially for the bromine atoms. The halogens are occupying nearly the same plane upward from the carbon; we can thus expect that the C−H axis is nearly aligned with the surface normal. This will be confirmed in the next section when the orientation of the molecule will be characterized.

The projection of the trajectory along the x and y axes, parallel to the surface plane (Figure 3), shows that the

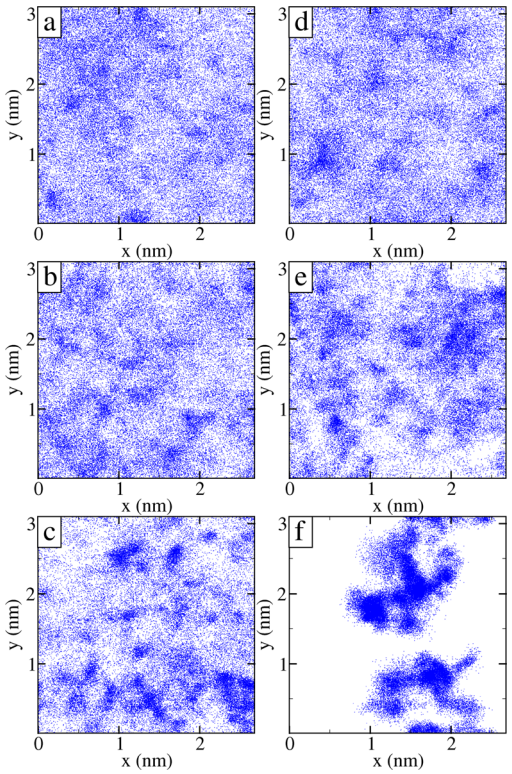

Figure 3. Diffusion of the halomethane parallel to the surface plane for (a) CH_3Cl, (b) CH_2Cl_2, (c) $CHCl_3$, (d) CH_3Br, (e) CH_2Br_2, and (f) $CHBr_3$. The blue dots represent the successive x and y positions of the carbon atom.

chloromethane and bromomethane have a significant mobility and can explore various adsorption sites while remaining adsorbed. CH_2Cl_2, CH_2Br_2, and $CHCl_3$ exhibit also significant surface diffusion motion (Figure 3b,e,c), but less homogeneous, because some preferential sites can be identified for CH_2Br_2 and $CHCl_3$ from the regions with high density plots. This is even more pronounced for $CHBr_3$ (Figure 3f), which appears to be confined in some regions of the surface with a reduced surface diffusion. This is the sign of a stronger binding of $CHBr_3$ to the surface layer than for the other compounds, as shown in part 4.

Finally, for all species, no diffusion through the ice layers is observed because only the outermost layer exhibits some substantial disorder. Getting closer to the melting temperature or performing the same calculations on a porous surface would of course promote diffusion through the ice lattice.

2. Orientation at the Surface. The snapshots shown in Figure 1 and the comparison of the carbon and halogen density profiles in Figure 2 already provide a rough idea of the orientation of the various admolecules at the ice surface, but it is nevertheless useful to investigate the surface orientation in a more quantitative way. Orientational distributions $P(\cos\theta)$ have been calculated, where θ is the angle between the interface normal (z-axis) and the molecular vector $\mathbf{v}$ whose definition varies with the different investigated halomethane compounds. These orientational distributions have been calculated separately for each interface. Figure 4 shows the distributions obtained for the upper interface.

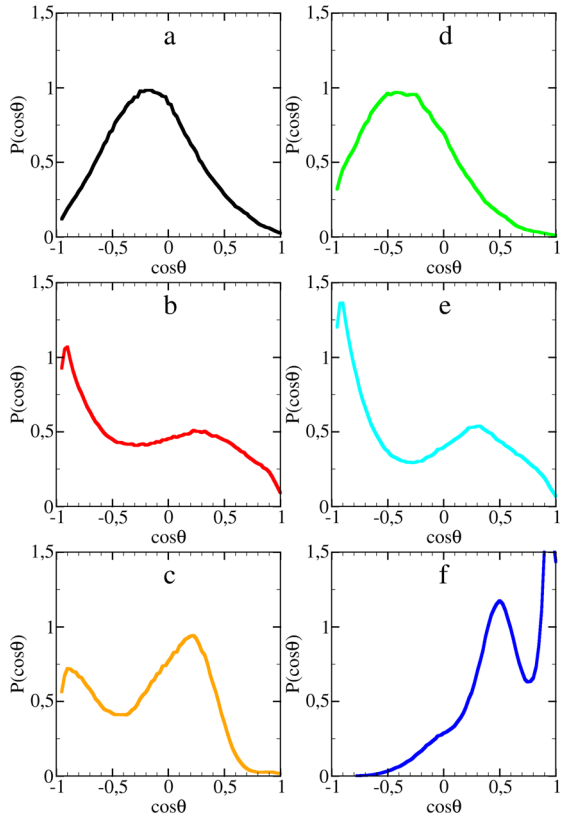

Figure 4. Orientation of the halomethane adsorbed on the ice surface. θ is the angle between the interface normal (z-axis) and the molecular vector $\mathbf{v}$. For the CH_3X molecules (X = Cl or Br) (a and d), the molecular vector points from the carbon atom C of the methyl group toward the halogen X, $\mathbf{v}$ = C → X. (2) For the CH_2X_2 species (b and e), the molecular vector is taken as one C−H bond. For the CHX_3 species (c and f), the molecular vector points from the carbon atom to the hydrogen, $\mathbf{v}$ = C → H.

For CH_3X (X = Cl or Br), the molecular vector $\mathbf{v}$ = X → C points from the halogen atom to the carbon atom. $\cos\theta = 0$ means that the CH_3X molecule is aligned with the C−X axis parallel to the surface, $\cos\theta = 1$ corresponds to the molecular axis oriented perpendicular to the surface with the halogen (X) atom pointing toward the ice layer, whereas $\cos\theta = -1$ denotes a perpendicular orientation of the molecular axis relative to the surface with the methyl group directed toward the gas phase. Panels a and d of Figure 4 represent the distributions calculated respectively for CH_3Cl and CH_3Br. Both angular distributions are similar and characterized by a single broad peak. The distribution is centered around $\cos\theta = -0.15$ for CH_3Cl and $\cos\theta = -0.4$ for CH_3Br, characteristic of a tilted orientation of the X−C axis of the chloromethane and bromomethane molecules at the angle $\theta = 99°$ and 113°, respectively, relative to the surface normal. CH_3Br molecule is thus slightly more tilted with respect to the normal to the surface than CH_3Cl, the hydrogens of the halomethane being directed toward the

DOI: 10.1021/acs.jpca.5b06071
J. Phys. Chem. A 2015, 119, 10052−10059

surface. This is fully consitent with the z density profiles previously described, characteristic of a flat configuration of the two halomethanes on the surface.

CH_2X_2 (X = Cl or Br) orientation is defined by the molecular vector $\mathbf{v}$ = C → H with taking into account only one of the two (equivalent) hydrogen atoms for the analysis. We note that the molecular vector defined using the other hydrogen atom (or both of them) would lead to an identical distribution. The orientational distributions obtained for both CH_2Cl_2 and CH_2Br_2 exhibit two peaks, for the same angle, corresponding to two possible orientations of one of the C−H bond. The maxima correspond to configurations where one C−H axis is directed toward the surface tilted by around 155° degrees with respect to the surface normal and the second one, where the same C−H bond is directed toward the gas phase (tilted by 72° from the surface normal). As a consequence, one of the halogens is pointing toward the gas phase and the second one toward the interface, as shown on Figure 1b,e.

Finally, for the trihalomethanes, we define the molecular vector $\mathbf{v}$ = C → H, i.e., from the carbon to the hydrogen atom. $CHCl_3$ and $CHBr_3$ differ strongly in their orientation as shown from the angular distributions (Figure 4c,f). The trichloromethane molecule orientational distribution (Figure 4c) is characterized by a broad peak centered around $\cos\theta = 0.3$ (θ = 72°) and by a second broad peak, less intense, for θ close to 180°, corresponding to the halogens directed toward the gas phase. The orientation obtained from our calculations is consistent with Aoki's experimental results,[14] showing that the $CHCl_3$ molecules are adsorbed on the topmost ice layer with their H atoms pointing toward the substrate at 35 K and with their Cl atoms away from the ice layers. The orientation of $CHBr_3$, shown in Figure 4f, is characterized by bimodal distribution with a broad peak centered around $\cos\theta = 0.4$ (θ = 66°) and a second peak, more intense, for $\cos\theta$ close to 1. For this latter orientation, the hydrogen is the only atom pointing toward the gas phase, the three bromine atoms facing the ice layer. The orientation of the tribromomethane is thus very different from its chlorinated analog, as illustrated on the snapshots shown in Figure 1 panels c and f. The orientation of these halocarbons has been characterized in a previous study at the air/liquid water interface by using the same semiempirical description.[18] For halomethanes, the orientations on liquid water and on ice are rather similar (even if broader at the liquid interface). By contrast, for CH_2Cl_2, $CHCl_3$, and CH_2Br_2, some preferential orientations are evidenced on ice. We should actually relate these differences to the temperature at which the simulations have been performed, 300 K for the liquid interface and 235 K for the ice surface. The thermal energy present for the liquid film calculations allows both the admolecules to adopt various orientations, and the interface to relax upon the adsorption of the haloalkane. As a result, the distributions at the liquid interface are smoothed out compared to the ones obtained for ice. For $CHBr_3$, the signature of two preferential orientations can also be distinguished, even if less pronounced, at the liquid interface, similarly to the ice surface.

1.3. Bonding Properties from Geometric Criteria. Figure 5 shows radial distribution functions (RDFs) $g(r)$ characterizing the bonding of the various halomethanes with the water molecules. The first interesting distance used in $g(r)$ is the distance between the halogen atom (X = Cl or Br) in the halomethane molecule and the hydrogen atoms (H) in the water molecules. These distributions are represented in Figure 5 for the halomethanes series. Except for CH_2Cl_2 and $CHCl_3$,

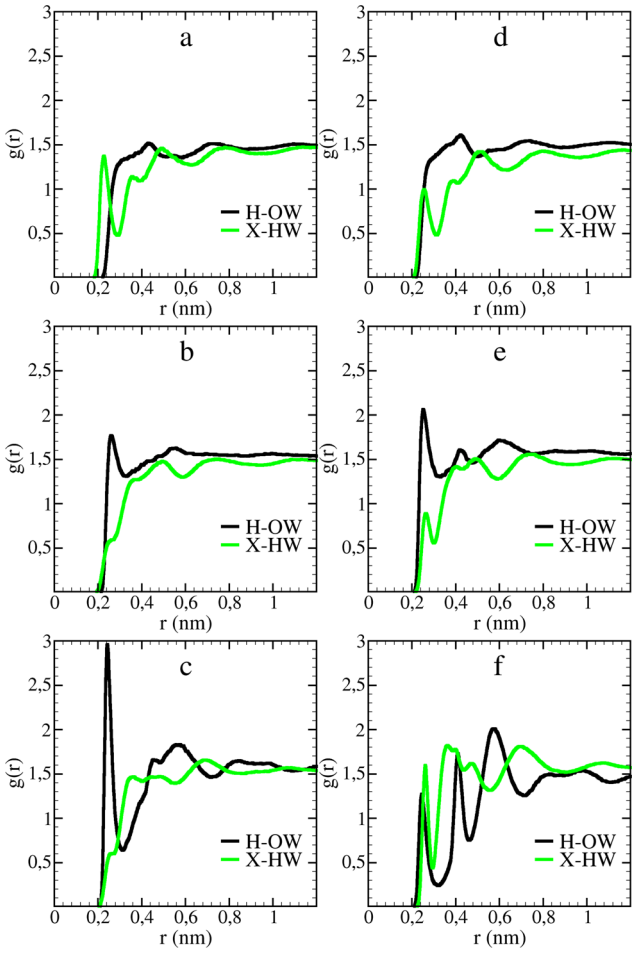

Figure 5. Radial distribution functions characterizing the X halogen atom(s) H atoms of water distance (green line) and H atom(s) of the halomethane oxygen atom of water distance (black line) respectively for (a) CH_3Cl, (b) CH_2Cl_2, (c) $CHCl_3$, (d) CH_3Br, (e) CH_2Br_2, and (f) $CHBr_3$.

the $g_{X\cdots Hw}(r)$ distributions are characterized by a pronounced peak for distances from 0.21 to 0.25 nm, indicating that the corresponding halomethane molecules bind to water through the formation of a X···H bond with unsaturated hydrogens of the surface layer. Halomethanes can also bind to the oxygen atom of water through their hydrogen atoms thanks to the polarity of the C−H bonds; this is characterized by the $g_{H\cdots Ow}(r)$ radial distribution. The $g_{H\cdots Ow}(r)$ distributions (Figure 5) exhibit peaks for H···O distances ranging between 0.2 and 0.25 nm for all species except for CH_3Cl and CH_3Br. Most of the species adopt orientations allowing the formation of weak hydrogen bonds between the halomethane hydrogens and unsaturated oxygen atoms of the surface. The orientation of $CHCl_3$ at the surface, with the hydrogen atom pointing toward the innerlayers, optimizes this type of binding. Among the series, CH_2Br_2 and $CHBr_3$ combine both types of bonding by forming Br···H_w and H···O_w bonds. This binding is possible thanks to the tilted orientation of the two molecules at the interface. When $CHBr_3$ is adsorbed with the hydrogen pointing straight to the gas phase ($\cos\theta = 1$), the formation of Br···H bonds is evidently favored in this case.

The orientation and bonding features obtained from our calculations indicate that, for all brominated halomethanes and for CH_3Cl, the bonding to the ice surface occurs mainly

DOI: 10.1021/acs.jpca.5b06071
J. Phys. Chem. A 2015, 119, 10052−10059

through the halogen atoms. For CH_2Cl_2 and $CHCl_3$, the chlorine atoms do not seem to be attached to a dangling H atom of the surface and point freely toward the gas phase. These results are in agreement with the IR investigation by Holmes et al.,[10] particularly for the brominated halomethanes, because they evidenced that in the series CBr_nH_{4-n}, with n = 1−4, the bonding to a 12 K amorphous ice film is through the bromine atom(s).

The differences we observe in the nature of the bonding of the studied halomethanes with the ice surface may be of importance regarding their photodissociation and the ability of the photoproducts, like the halogen radicals, to be released in the gas phase or trapped at the surface.

1.4. Interaction Energy. The strength of the interaction of the admolecule with the ice surface is also an important parameter that can be compared with experiments. From the MD simulations, the short-range interaction energy can be obtained and averaged over the simulation time. The total short-range interaction energy is calculated as a sum of the short-range dispersion−repulsion and electrostatic contributions. The long-range correction of the interaction between the admolecule and the surface cannot be distinguished from all the interactions, including the water−water interaction, with using the PME summation method. Still, the comparison between the short-range adsorption energies of the various haloalkanes provides a useful qualitative description of the relative strength of the binding. The general observations that can be addressed from the energy distributions given in Figure 6 are the following: (i) the strength of the interaction increases with the number of halogen substituents, (ii) the distribution gets also broader as the number of halogens is increasing, and (iii) the bromine compounds exhibit larger adsorption energies than their chlorinated analogs. For all the studied adsorbates, the electrostatic contribution is dominating with its average ratio ranging from 51% ($CHCl_3$) to 76% ($CHBr_3$) of the total short-range halomethane-ice interaction energy.

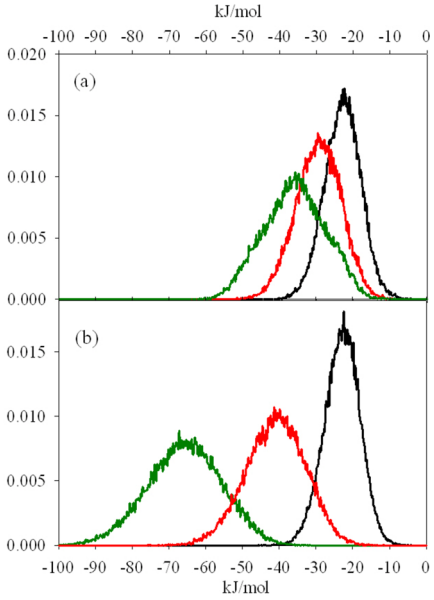

Figure 6. Energy distribution (kJ/mol) for the total short-range interaction energy between the ice surface and CH_3X (black curve) or CH_2X_2 (red curve) or CHX_3 (green line) with (a) X = Cl and (b) X = Br.

CH_3Cl exhibits the weakest interaction (−22 kJ/mol) and the interaction is increasing from CH_2Cl_2 (−30 kJ/mol) to $CHCl_3$ (−38 kJ/mol). The distribution in energy for CH_3Br is slightly narrower than the one of CH_3Cl but with a comparable value for the maximum (−22 kJ/mol). Because CH_2Br_2 is forming both Br···H(water) and H···O(water) bonds, it has a larger interaction, by about 10 kJ/mol, with the water ice than CH_2Cl_2. As supposed from the mobilities of the admolecules (Figure 3 and part 1.1), the strongest adsorption energy (−70 kJ/mol) is obtained for tribromomethane, twice larger than the $CHCl_3$ one, certainly because of the formation of Br···H(water) bond. The present comparison agrees well with the experimental results of Grecea et al.,[15] who concluded from their desorption temperature that $CHBr_3$ is more strongly bound to ice than $CHCl_3$, but the agreement is only limited to this property. Actually, they also observed a lower barrier for surface diffusion of $CHBr_3$ on ice compared to that for $CHCl_3$, which is in contradiction with the binding strength they suppose and our results presented previously (Figure 3). To resolve this ambiguity, the diffusion of the trihalogenated compounds would need to be investigated in more detail on a defective surface to allow the molecules to percolate throught defects (cracks, grains boundaries) in the ice lattice.

Finally, the trend we observe on the bonding properties can be compared with studies of the hydrogen bonding between chlorinated methanes and the oxygen atom of liquid water dimers by Hobza and co-workers.[16] They found that the interaction energy increased in the order CCl_4 > $CHCl_3$ > CH_2Cl_2 > CH_3Cl, the order being consistent with our results.

■ CONCLUSION

This MD study addresses a detailed analysis of the adsorption properties of a single halomethane molecule $CH_{4-n}X_n$, n = 1−3, X = Cl, Br at the air/ice interface at the nominal temperature of 235 K that corresponds to 15 K undercooling relative to the melting point of the water model employed. All of the studied molecules remain adsorbed at the surface during the entire 50 ns simulation runs. The surface orientation of the admolecules varies from one species to another and as a result the bonding properties of the individual admolecules are also slightly different. No substantial difference is observed for the orientation of the studied molecules at the air/ice interface in comparison with the orientation at the air/water interface except that the more structured character of the ice surface compared to that of a liquid supports several more pronounced preferential orientations. We might expect more differences for lower temperatures because the simulations have been carried out close to the melting point (15 K undercooling) to mimic the tropospheric conditions. In general, the adsorbate binds to water through either the halogen (X···H_w) or the hydrogen (H···O_w) atoms. The interaction energy, mainly electrostatic in nature, is increasing with the number of halogen substituents, the brominated compounds showing significantly stronger interactions than their chlorinated analogs. The range of the interactions is qualitatively consistent with previous experimental data.

$CHBr_3$ and CH_2Br_2, known as VSLS, are produced in principle in the troposphere. The present study shows that these two species may stick to the ice surface. We can thus propose that upon adsorption on ice particles, they may be able to reach higher altitudes and contributing to stratospheric bromine loading.

DOI: 10.1021/acs.jpca.5b06071
J. Phys. Chem. A 2015, 119, 10052−10059

Another important result is that the halogen atoms of the monochloro or monobromomethane are clearly pointing toward the gas phase, making it easily releasable upon photodissociation; for the disubstituted species, even if one halogen is embedded in the ice lattice, the second one is also directed to the vapor phase. The same trend is observed for $CHCl_3$. By contrast, $CHBr_3$ is adsorbed with having the three halogens encapsulated in the ice, making them less available for reactions with gas phase species or less releasable in the gas phase upon photodissociation. As a consequence, the adsorption of these species at the ice surface may alter their photodissociation properties and the direct release of the photoproducts.

AUTHOR INFORMATION

Corresponding Author

*C. Toubin. E-mail: celine.toubin@univ-lille1.fr.

Present Address

PhLAM Laboratory, UMR CNRS 8523, Université de Lille, Cité Scientifique, 59655 Villeneuve d'Ascq, France.

Author Contributions

The manuscript was written through contributions of all authors. All authors have given approval to the final version of the manuscript.

Funding

Czech Science Foundation (Grant 13-06181S), Institute of Organic Chemistry and Biochemistry (AS CR via RVO 61388963), PHC-Barrande (26513PA) funded by the french Ministry of Foreign Affairs and the Czech Ministry of Education, the CaPPA project (Chemical and Physical Properties of the Atmosphere) funded by the French National Research Agency (ANR) through the PIA (Programme d'Investissement d'Avenir) under contract ANR-10-LABX-005, CNRS and Université Lille 1.

Notes

The authors declare no competing financial interest.

ACKNOWLEDGMENTS

The authors thank Ivan Gladich and Pavel Jungwirth for helpful discussions. Access to computing and storage facilities owned by parties and projects contributing to the National Grid Infrastructure MetaCentrum, provided under the programme "Projects of Large Infrastructure for Research, Development, and Innovations" (LM2010005), is greatly appreciated.

REFERENCES

(1) Saiz-Lopez, A.; von Glasow, R. Reactive halogen chemistry in the troposphere. *Chem. Soc. Rev.* **2012**, *41* (19), 6448−6472.

(2) Abbatt, J. P. D.; et al. Halogen activation via interactions with environmental ice and snow in the polar lower troposphere and other regions. *Atmos. Chem. Phys.* **2012**, *12* (14), 6237−6271.

(3) Aschmann, J.; Sinnhuber, B. M. Contribution of very short-lived substances to stratospheric bromine loading: uncertainties and constraints. *Atmos. Chem. Phys.* **2013**, *13* (3), 1203−1219.

(4) Hossaini, R.; et al. Growth in stratospheric chlorine from short-lived chemicals not controlled by the Montreal Protocol. *Geophys. Res. Lett.* **2015**, *42*, 42.

(5) Karlsson, A.; Theorin, M.; Abrahamsson, K. Distribution, transport, and production of volatile halocarbons in the upper waters of the ice-covered high Arctic Ocean. *Global Biogeochemical Cycles* **2013**, *27* (4), 1246−1261.

(6) Verhulst, K. R.; Aydin, M.; Saltzman, E. S. Methyl chloride variability in the Taylor Dome ice core during the Holocene. *J. Geophys. Res.: Atmos.* **2013**, *118* (21), 12218−12228.

(7) Saltzman, E. S.; Aydin, M.; Tatum, C.; Williams, M. B. 2,000-year record of atmospheric methyl bromide from a South Pole ice core. *J. Geophys. Res.: Atmos.* **2008**, *113* (D5), D05304.

(8) Harper, K.; Minofar, B.; Sierra-Hernandez, M. R.; Casillas-Ituarte, N. N.; Roeselova, M.; Allen, H. C. Surface residence and uptake of methyl chloride and methyl alcohol at the air/water interface studied by vibrational sum frequency spectroscopy and molecular dynamics. *J. Phys. Chem. A* **2009**, *113* (10), 2015−2024.

(9) Rowland, F. S. Stratospheric ozone depletion. *Philos. Trans. R. Soc., B* **2006**, *361*, 769−790.

(10) Holmes, N. S.; Sodeau, J. R. A Study of the Interaction between Halomethanes and Water-Ice. *J. Phys. Chem. A* **1999**, *103*, 4673−4679.

(11) Vysokikh, T. A.; Mukhamedzyanova, D. F.; Yagodovskaya, T. V.; Savilov, S. V.; Lunin, V. V. The interaction of CH3Cl, CH2Cl2, CHCl3, and CCl4 with ozone on the surface of ice under stratospheric conditions. *Russian Journal of Physical Chemistry A* **2007**, *81* (11), 1836−1839.

(12) Cyriac, J.; Pradeep, T. Probing Difference in Diffusivity of Chloromethanes through Water Ice in the Temperature Range of 110−150 K. *J. Phys. Chem. C* **2007**, *111*, 8557−8565.

(13) Schaff, J. E.; Roberts, J. T. Toward an Understanding of the Surface Chemical Properties of Ice: Differences between the Amorphous and Crystalline Surfaces. *J. Phys. Chem.* **1996**, *100*, 14151−14160.

(14) Aoki, M.; Ohashi, Y.; Masuda, S. Interactions of CHCl3 molecules with a crystalline ice grown on Pt(111) studied by metastable impact electron spectroscopy. *Surf. Sci.* **2003**, *532*−*535*, 137−141.

(15) Grecea, M. L.; Backus, E. H. G.; Fraser, H. J.; Pradeep, T.; Kleyn, A. W.; Bonn, M. Mobility of haloforms on ice surfaces. *Chem. Phys. Lett.* **2004**, *385* (3−4), 244−248.

(16) Hobza, P.; Sandorfy, C. Quantum chemical and statistical thermodynamic investigations of anesthetic activity. The interaction between CH4, CH,Cl, CH2C12, CHCI,, CCl, and an O-H.. -O hydrogen bond. *Can. J. Chem.* **1984**, *62*, 606.

(17) Wang, W.; Tian, A.; Wong, N. B. Theoretical Study on the Bromomethane-Water 1:2 Complexes. *J. Phys. Chem. A* **2005**, *109*, 8035−8040.

(18) Habartova, A.; Valsaraj, K. T.; Roeselova, M. Molecular dynamics simulations of small halogenated organics at the air-water interface: implications in water treatment and atmospheric chemistry. *J. Phys. Chem. A* **2013**, *117* (38), 9205−9215.

(19) Abascal, J. L. F.; Vega, C. A general purpose model for the condensed phases of water: TIP4P/2005. *J. Chem. Phys.* **2005**, *123*, 234505.

(20) Buch, V.; Sandler, P.; Sadlej, J. Simulations of H2O Solid, Liquid, and Clusters, with an Emphasis on Ferroelectric Ordering Transition in Hexagonal Ice. *J. Phys. Chem. B* **1998**, *102*, 8641−8653.

(21) Bernal, J. D.; Fowler, R. H. A Theory of Water and Ionic Solution, with Particular Reference to Hydrogen and Hydroxyl Ions. *J. Chem. Phys.* **1933**, *1*, 515.

(22) Berendsen, H. J. C.; Postma, J. P. M.; van Gunsteren, W. F.; DiNola, A.; Haak, J. R. Molecular dynamics with coupling to an external bath. *J. Chem. Phys.* **1984**, *81* (8), 3684−3690.

(23) Vega, C.; Martin-Conde, M.; Patrykiejew, A. Absence of superheating for ice Ih with a free surface: a new method of determining the melting point of different water models. *Mol. Phys.* **2006**, *104* (22−24), 3583−3592.

(24) Bussi, G.; Donadio, D.; Parrinello, M. Canonical sampling through velocity rescaling. *J. Chem. Phys.* **2007**, *126*, 014101.

(25) Hess, B.; et al. GROMACS 4: Algorithms for highly efficient, load-balanced, and scalable molecular simulation. *J. Chem. Theory Comput.* **2008**, *4* (3), 435−447.

(26) Hockney, R. W.; Goel, S. P.; Eastwood, J. W. Quiet high-resolution computer models of a plasma. *J. Comput. Phys.* **1974**, *14* (2), 148−158.

DOI: 10.1021/acs.jpca.5b06071
J. Phys. Chem. A 2015, 119, 10052−10059

(27) Darden, T.; York, D.; Pedersen, L. Particle Mesh Ewald - an N.Log(N) Method for Ewald Sums in Large Systems. *J. Chem. Phys.* **1993**, *98* (12), 10089−10092.
(28) Essmann, U.; Perera, L.; Berkowitz, M. L.; Darden, T.; Lee, H.; Pedersen, L. G. A Smooth Particle Mesh Ewald Method. *J. Chem. Phys.* **1995**, *103* (19), 8577−8593.
(29) Miyamoto, S.; Kollman, P. A. SETTLE: An analytical version of the SHAKE and RATTLE algorithm for rigid water models. *J. Comput. Chem.* **1992**, *13*, 952−962.
(30) Humphrey, W.; Dalke, A.; Schulten, K. VMD - Visual Molecular Dynamics. *J. Mol. Graphics* **1996**, *14*, 33−38.

DOI: 10.1021/acs.jpca.5b06071
J. Phys. Chem. A 2015, 119, 10052−10059